Chapter 16

Engineering geology, rock mechanics and rock engineering for the design and construction of underground (UNPP) rock caverns

16.1 Introduction

The objective of this chapter is to assist in the understanding of some basic rock mechanics and rock engineering principles which are needed following the site investigation for a future underground nuclear power plant development. We will also refer to some prior rock engineering experiences selected from Norway, Taiwan and China which illustrate the confidence with which we have utilized the underground for the construction of large caverns, especially in the last three decades. A variety of rock mass qualities will be referred to, not just the jointed pre-Cambrian granitic gneiss for the widest 60m span, but also far from ideal volcanic extrusive columnar basalts for huge pairs of twin hydropower caverns, and caverns in challenging interbedded sandstone with faulted (sheared) clay inter-beds. The siting needs in these particular cases vary very widely: a convenient city-outskirts hillside, a major river canyon dam site for hydropower, and a far from ideal underground rock cavern site but with the advantages of an existing top-reservoir for pumped hydro. Due to the huge range of sites utilized in the past decades, we have learned how to safely engineer the necessary cavern complexes in geologic locations that may not always be ideal from a rock mass quality viewpoint. Important developments have occurred and been applied during at least the last six decades, that make use of the underground something approaching a routine exercise for numerous countries. This is because of the expertise and long experience of hundreds of site investigation, design, consulting and contracting companies operating in the many countries regularly making these underground developments, mostly since the nineteen sixties and seventies.

Besides the construction of tens of thousands of large-span tunnels for motorways and twin-track high-speed rail in numerous countries, we can by now count some 800 underground cavern complexes for hydropower world-wide. These need twinned machine hall and parallel transformer hall caverns, utilizing spans that have gradually increased from roughly 18m up to 34m and with cavern lengths from roughly 80m to 400m, keeping pace with the increased size and numbers of turbine units installed. The largest turbine units have now reached 1000Mw (Baihetan, China). The fact that the number of such underground facilities has grown from 200 some 30 years ago, to 800 today is practical evidence of both the needs and the world’s collective rock engineering abilities. Norway was once the operator of 75% of these power plants. This has changed completely since Norway virtually completed its renewable power supply.

The tragic consequences of the Fukushima tsunami accident means that the seashore or remote river sites for cooling water may need substitution by isolated cooling water lagoons: a principal that has been in use so long that surface plants with such cooling-water facilities have by now been decommissioned after 50 years of continuous nuclear power production. If we used tunneled water from such lagoons, we would not need to be challenged by the potential variability of sea level or river level cooling, with their clear environmental and occasionally dramatic safety issues.

16.2 Site investigation preliminaries

This chapter provides an over-view of typical construction-in-rock techniques, and will focus on illustration more than detailed description, in order to aid in rapid communication. We will address just the 'geo' aspects, based on the assumption that planners, local communities and local authorities, and not least nuclear engineers, have by now presented their finally approved plans and requirements for a potential underground siting of a suitably modified nuclear power plant. Of necessity this will be with associated turbine halls and cooling water tunnels, plus the dedicated transformer and transmission facilities of a multi-thousand Megawatt power plant. Other authors have addressed some of these 'non-geo' details in other chapters of this ISRM book.

The 'easier' part is actually the construction of the space required for a UNPP in a secured in-rock location. It is the easier part because the creation of major space underground has been done so many times before. For instance, oil storage caverns which reached 2,000,000m^3 of cavern storage space five decades ago, notably in Finland, Sweden and Norway, have now reached a staggering 8,000,000m^3 in the Middle East and involve almost 20km of parallel, radiator-like large-cavern constructions.

During the construction phase, though not thereafter, the chief challenge has proved to be ventilation, due to the drill-and-blast excavation needed with harder rock. An unnecessary modern challenge has also been arguments about the most suitable numerical modelling of stability aspects. In fact stability is not in doubt due to prior empirically-based support routines that the youngest generation of rock engineers are poorly informed about, due to their 'modelling' education by not quite old enough numerically proficient professors.

With potential sites identified by planners, following a no doubt lengthy process of lobbying and tax benefit guarantees (among much else), we may finally arrive at the stage where the 'geo' professions get to apply their varied expertise. *Geologists, structural geologists, geophysics specialists, and then site investigation companies specializing in core-drilling, permeability measurement and down-hole logging*, are the successive disciplines needed at this early stage. This is followed by *engineering geologists* who utilize each of the above sets of skills and data, and combine them with *rock mass characterization* and *rock sample and rock joint sample testing*. Much of the

above may be used directly in *empirical tunnel and cavern design routines*, but for sure will be utilized in *numerical modelling to verify empirical designs*. However, we need to insist on relevant *discontinuum modelling*, not the colourful and less meaningful isotropic continuum modelling, with the questionable focus on so-called 'plastic' behaviour. Penultimately, we have the *tunnelling and rock cavern contractors*, followed by the *nuclear plant engineering specialists* for the very numerous and critical installation tasks.

The reality of rock engineering is that jointed rock of reasonable competence reacts to tunnel and cavern excavation, if at moderate depth, by changes of stress and resulting strain, so there are small, accumulated displacements that are also contributed to by rock joint deformations which include minor amounts of shearing, joint opening, and some closing. We do not need to call this 'plastic' behaviour. Typical hard rock is very far from squeezing or failing by shearing, as the modeller's 'plastic' term might imply.

The deformations and joint adjustments are limited by rock mass reinforcement to some minor extent, but since the rock mass is bearing the majority of the physical consequences of tunnel or cavern excavation, the efforts we make to support and reinforce with shotcrete, sometimes concrete, and usually rock bolts, are more a guarantee of excavation stability. We cannot hinder stress redistribution. The latter is inevitable and needed, to generate a stable rock arch above any given excavation.

16.3 Geological and structural geological aspects

Two good examples of geological detail provided at different scales are illustrated in Figures 16.1 and 16.2 (permissions needed for ISRM book).

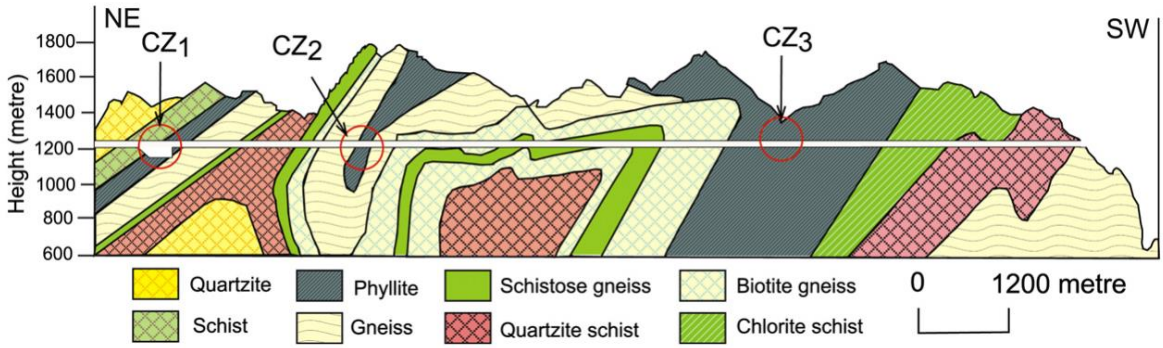

Figure 16.1 Selected due to the clarity of the objective. This is a geologic longitudinal section for a headrace tunnel in India, from Panda et al. 2014. The various rock types expected to be encountered could be based on the geologic interpretation of drill-core and on logging of surface exposures since some are steep enough to be partly free of vegetation. Such longitudinal sections can of course be updated and corrected following project completion,

While we can consider that the 'geology' provides knowledge of the rock types likely to be encountered underground, there may be an even greater need for structural

geological information. This will include large-scale lineations in the terrain, which are best studied with air-photo analysis of adjacent stereo pairs. (An index figure at the same location on adjacent air-photos assists the observer to see in 3D with the help of simple glasses, giving an optical result as if suddenly in a helicopter). Significant lineations, drawn with solid or tentative dotted lines can be drawn on plastic over-lays, and thence transferred to the geological plans. These help in the production of the all-important longitudinal sections showing the expected geology (and major fault zones) along the selected sections, and of course usually, and ideally, allow such features to be avoided for the planned (soon-to-be UNPP) cavern locations. On a more detailed scale the distinct joint-set orientations will be plotted as joint poles on lower-hemisphere Schmidt nets. An example is given later.

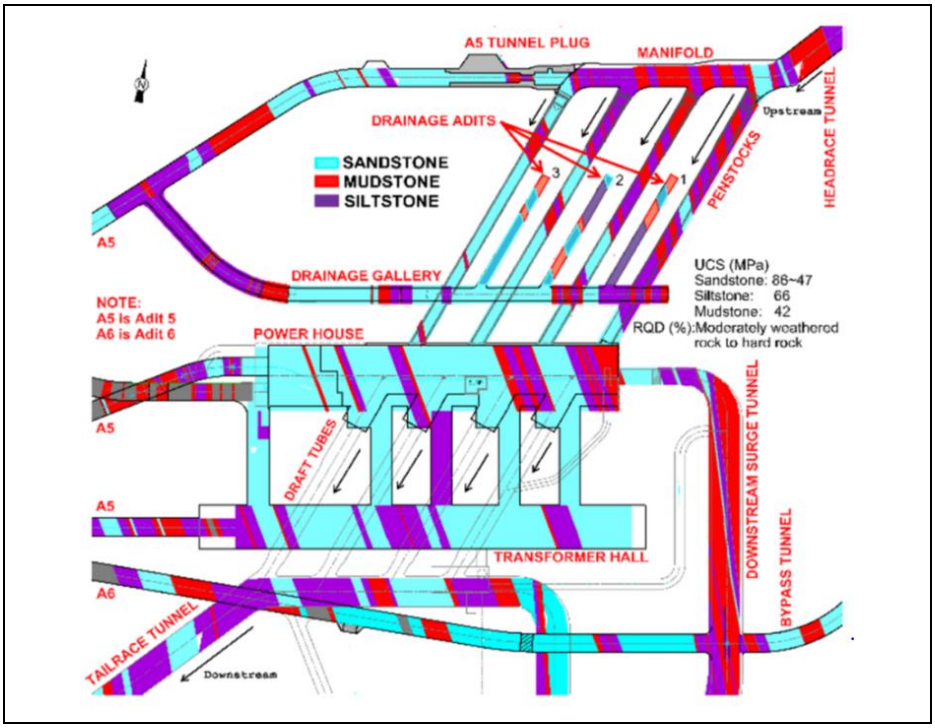

Figure 16.2 The distribution of rock types for the case of a hydropower cavern complex. Note the less-than-ideal sedimentary rock types: sandstone, mudstone and siltstone, but with the powerhouse and transformer halls located in the usually most competent of the three rock types. This level of geologic detail is likely to be at a reduced level prior to construction, but with sufficient numbers of non-vertical drill-holes and drill-core analysis, such projections might be possible. In a small inset on the right, a helpful UCS (unconfined compression strength) overview is given. The RQD % (rock quality designation) will have varied widely in the three rock types and is given elsewhere. From Rehman et al, 2021.

16.4 Seismic refraction measurements

Before drilling of boreholes for rock-core recovery and down-hole permeability testing it is essential and cost-saving to engage the services of a geophysics company for measurement of the seismic velocities in the rock masses overlying the planned rock cavern complexes. In fact, the order should be reversed to insist that before locating

the cavern complexes the rock masses available at the site should be measured with both seismic and resistivity measurements. The former, providing as a minimum the compressional P-wave velocity gives an almost immediate link to rock mass quality following density and uniaxial compression strength testing. The latter gives an indication of water content, porosity and maybe clay. The drilling of boreholes for core samples, down-hole testing and laboratory testing is the next stage, to be guided by the velocity distributions. For example, where lower velocities are indicated, inclined boreholes will be drilled to sample some of the lower velocity zones, as here there would be slower tunnelling progress and more rock support.

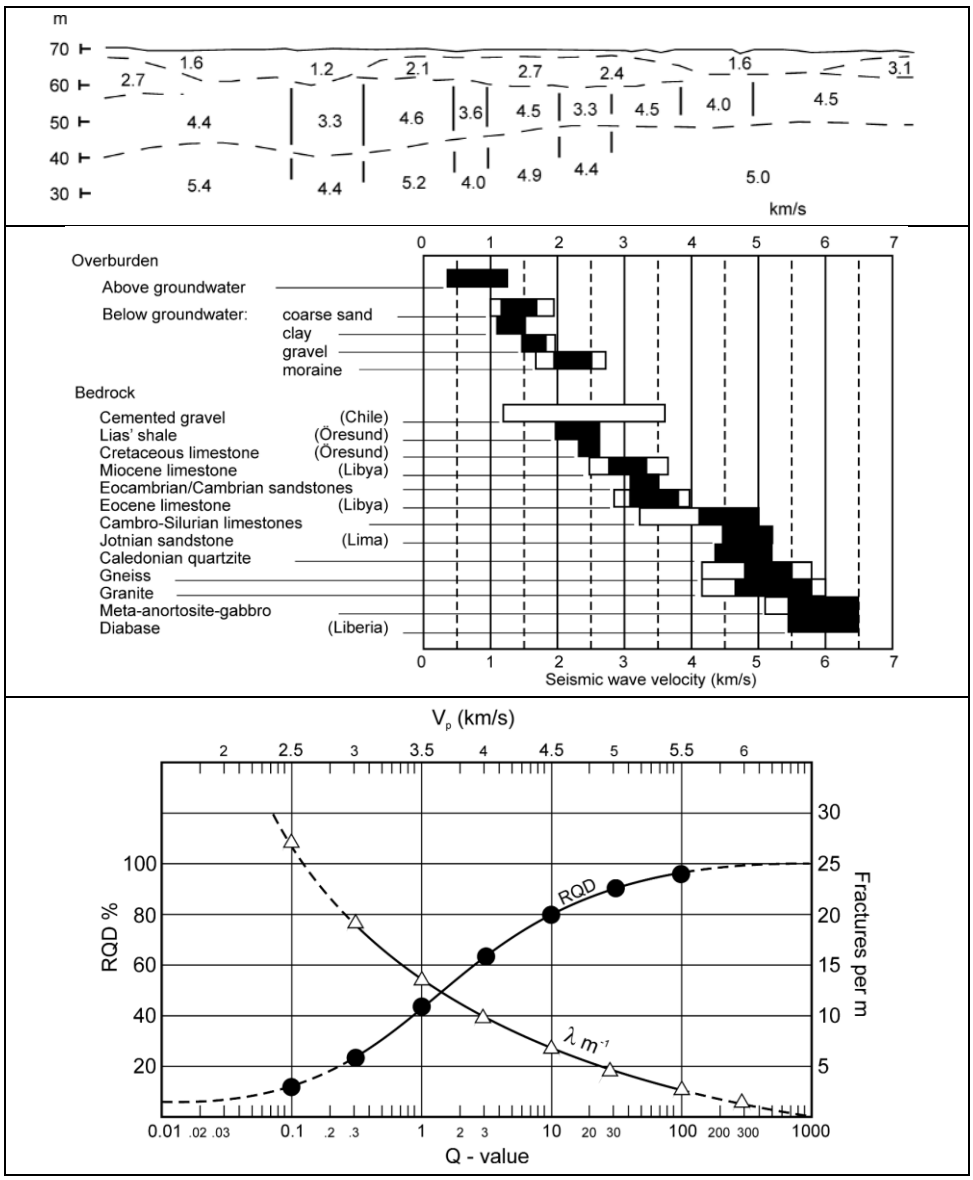

Figure 16.3 A convenient three-stage velocity interpretation diagram. a) Seismic refraction section of some 200m length (Many kilometers will be needed). b) Some typical interpretations of potential rock types to be corrected or reinforced by the geologic longitudinal section. c) Preliminary link of velocity to RQD (% of core pieces > 10cm length), to joint frequency per meter (λ m^{-1}), and to the rock mass quality Q-value if hard rock. Q will be introduced shortly and a more advanced velocity interpretation will be shown with ad justments for depth or stress. From Sjøgren et al. 1979 and Barton, 1995, 2006.

16.5 Drill-core and permeability measurements

Low velocity zones, faults, and *potentially favourable* geologies would be drilled for core-recovery and rock / rock joint sampling, with drilling locations and inclinations (from the standard vertical) assisted by the seismic and resistivity surveys performed. This will be the stage for temporary access roads to be established in the terrain, assuming the site is partly remote, although caterpillar-mounted drill rigs are common.

Figure 16.4 Part of the Swedish SKB core shed at Forsmark, used for analysing and logging numerous 1000m deep boreholes for the planned HLW repository. A similar dedicated core-logging set-up will be an expected part of the site investigations for a UNPP. As expected, the rock mass quality at Forsmark, as seen here, is mostly very good, with high Q-values. There are a limited number of more fractured zones which have lower Q-values and therefore more easily measured permeability. (Fractured zones would be pre-injected with micro-cement grouts and silica-fume in any parts of the UNPP with probe-hole measured leakages above 'dripping' categories).

Figure 16.5 The contrasting very poor quality of a clay-bearing fracture zone in BH 741 at the 20km long four-TBM Follobanen rail project in Norway. Depth of core-box: 57 to 64m. The borehole is inclined, and the weakness zone is sub-vertical, with low P-wave velocity.

Many kilometres of refraction seismic profiles were 'shot' at this project in order to study the distribution of both low and high velocity zones within the mostly good (Q = 10-40) quality of the majority of the planned TBM tunnels. In the case of TBM operations the high velocities caused increased cutter wear and damage to bearings. For drill-and-blast tunnelling and cavern construction, as for an UNPP, high velocities mean less support, and lower permeability.

Concerning permeability and its measurement down-hole using straddle-packers and injection or pumping-out of water, it is found that the Lugeon value in litres/min/meter per 1MPa excess pressure often shows an approximate and rather simple relation to P-wave velocity and to rock quality (described by Q in next section).Table 16.1 gives a 'rule-of-thumb expectation of what to expect in approximate terms. This table of 'expectations' is useful because when a site shows lower or perhaps higher permeabilities than suggested in the table it may mean that respectively clay-filled or eroded/outwashed discontinuities are present in the test zones.

Table 16.1 A set of inter-related geotechnical approximations that are useful when assessing velocity and permeability results in the field. Note: $Q_c = Q \times \sigma_c/100$. Barton, 2002, 2006.

Q_c	0.1	1	10	100
Lugeon	10	1	0.1	0.01
K (m/s) ≈	10^{-6}	10^{-7}	10^{-8}	10^{-9}
V_p (km/s)	2.5	3.5	4.5	5.5

16.6 Analysing rock mass quality with the Q-system

There are various ways to describe the quality of rock masses. Some countries have their own special systems, even with differing systems for the road and rail authorities (Japan). In Norway we developed the Q-system 45 years ago, and it has steadily gained in use around the world. It combines rock mass quality description (using six parameters) with estimation of suitable tunnel and cavern support and reinforcement. The latter will be illustrated later. Q is preferred to another 'international' method RMR from Bieniawski, 1989 because it is more specifically depth, stability, tunnel (and cavern) support and over-break oriented, and is linked to other parameters such as P-wave velocity and deformation modulus (E_{mass} or M). The latter applies to RMR also, and a combined Q-RMR-E_{mass} estimation will be shown later, ahead of the section on numerical modelling. A deliberate non-selection of Hoek's GSI is made as this 'picture-recognition' method has too many exceptions and is unfortunately linked to unrealistic numerical continuum modelling via remarkably complex equations.

The Q-system can be used in various ways when planning and executing tunnel and cavern projects. We can log drill-core with Q-histograms (Figure 16.7), relate Q to V_P when interpreting seismic refraction results (see later figure), log Q at the tunnel front

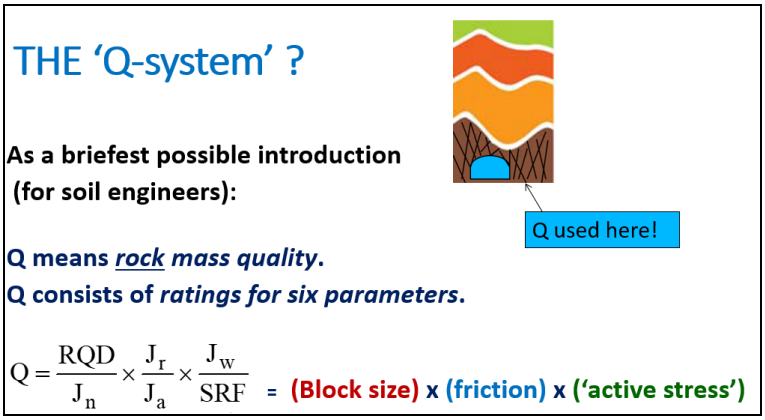

Figure 16.6. Basic elements of the Q-system. Six parameters are used in civil engineering applications for tunnel and cavern design and for construction follow-up. The first four parameters, which basically describe relative block-size and inter-block friction are widely used in the mining industry for the dimensioning of large stopes, and for stability or instability prediction.

	BRAZILIAN HYDROPOWER PROJECT COLLAPSE IN FAULTED ZONE *LOWEST END OF THE ROCK MASS QUALITY SCALE. (Inadequate support).* Q ≈ 10/20 x 1/8 x 0.5/20 **Q < 0.001**
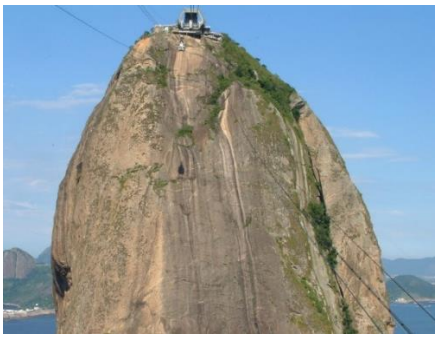	SUGAR LOAF MOUNTAIN, RIO DE JANEIRO *TOP END OF ROCK MASS QUALITY SCALE. (No support would be needed).* Q ≈ 100/0.5 x 4/0.75 x 1/1 **Q >1000**

Figure 16.7 Examples of the 'end-members' of rock mass quality according to Q. The six orders of magnitude range of quality illustrated correlates in a simple way with P-wave velocity, deformation modulus, permeability (the latter needing a modification for clay-filled joints, which reduce quality and permeability).

or in the rock cavern top-heading and arch to assist in rock mass reinforcement and support (see later figure), and estimate deformation modulus, and deformation, for numerical modelling (see later figures). All the above possibilities have been derived by empirical trial-and-error or *a posteriori* based on practice, not the 'popular' *a priori* based on assumptions option.

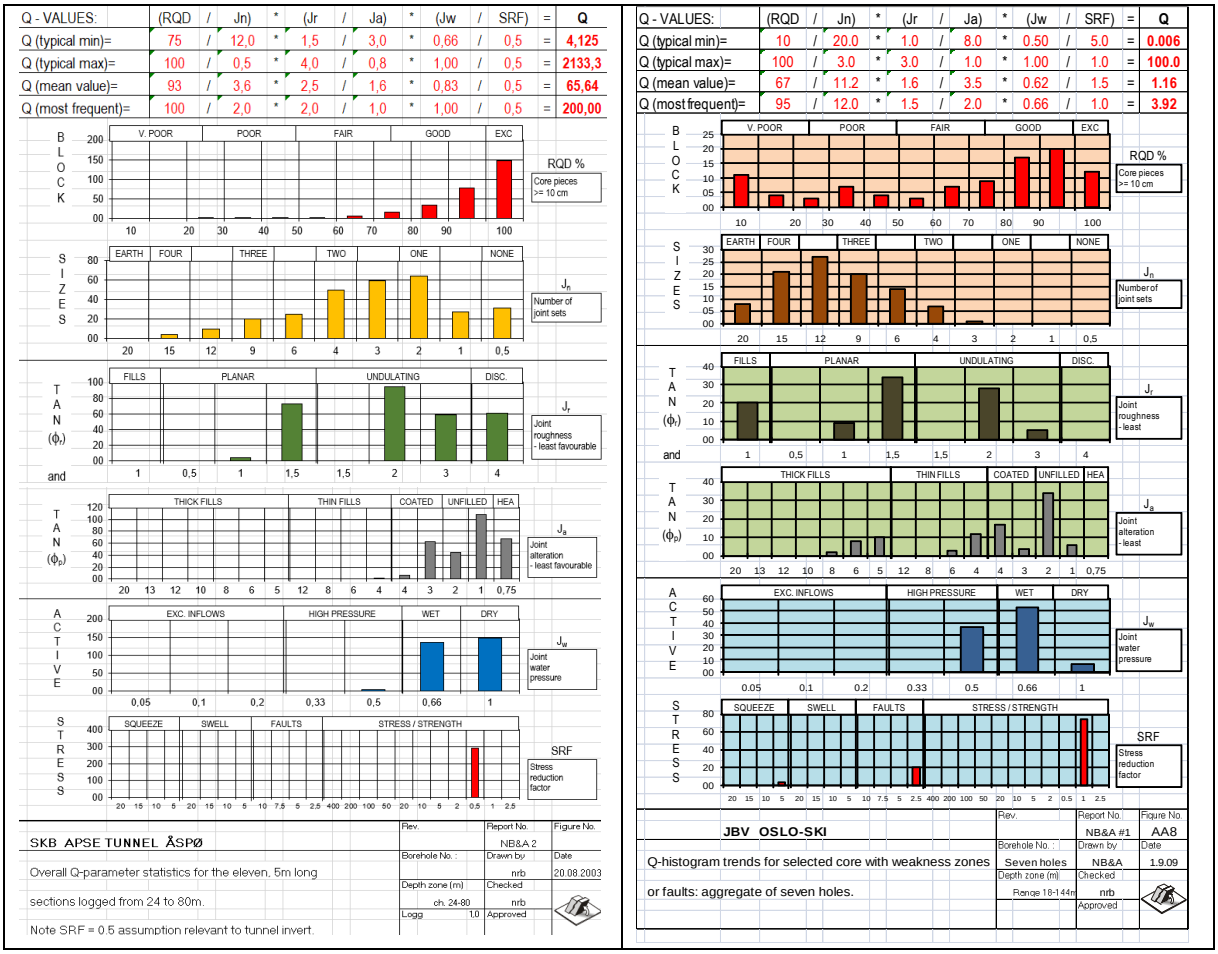

Figure 16.8 The six Q-parameters introduced in Figure 16.6 are illustrated here by means of frequency of observation histograms. The ratings beneath each parameter corresponds to the abbreviated descriptions above each parameter. On the left is the final result of logging inside an experimental excavation in SKB's Äspö pillar experiment APSE. The rock mass quality is most frequently an excellent Q =200. By contrast, and showing Q-parameter ratings plotting more to the left-hand-side, are the combined result of weakness zones, like Figure 16.5 which were sampled by drilling into low P-wave velocity areas of the seismic refraction profiles, such as those illustrated in Figure 16.3a.

Figure 16.3c provided a preliminary look at the potential relationship between the shallow refraction seismic velocity and measures of rock quality such as RQD (rock quality designation: % pieces of drill-core > 10cm in length) and joint frequency and the Q-value. This works reasonably well for hard non-porous rocks at shallow depth such as 20 to 40m. A more generalized result based on a much wider data base including cross-hole tomography to 1000m depth with adjacent Q-logging of the recovered core, is shown in Figure 16.9a. (See Barton, 2006 for descriptions of the data base). This combines velocity correction for depth (+ve) and porosity (-ve) and the application of a more widely applicable Q_c (=Q x σ_c/100) where σ_c is the unconfined compression strength of the rock, commonly referred to as UCS.

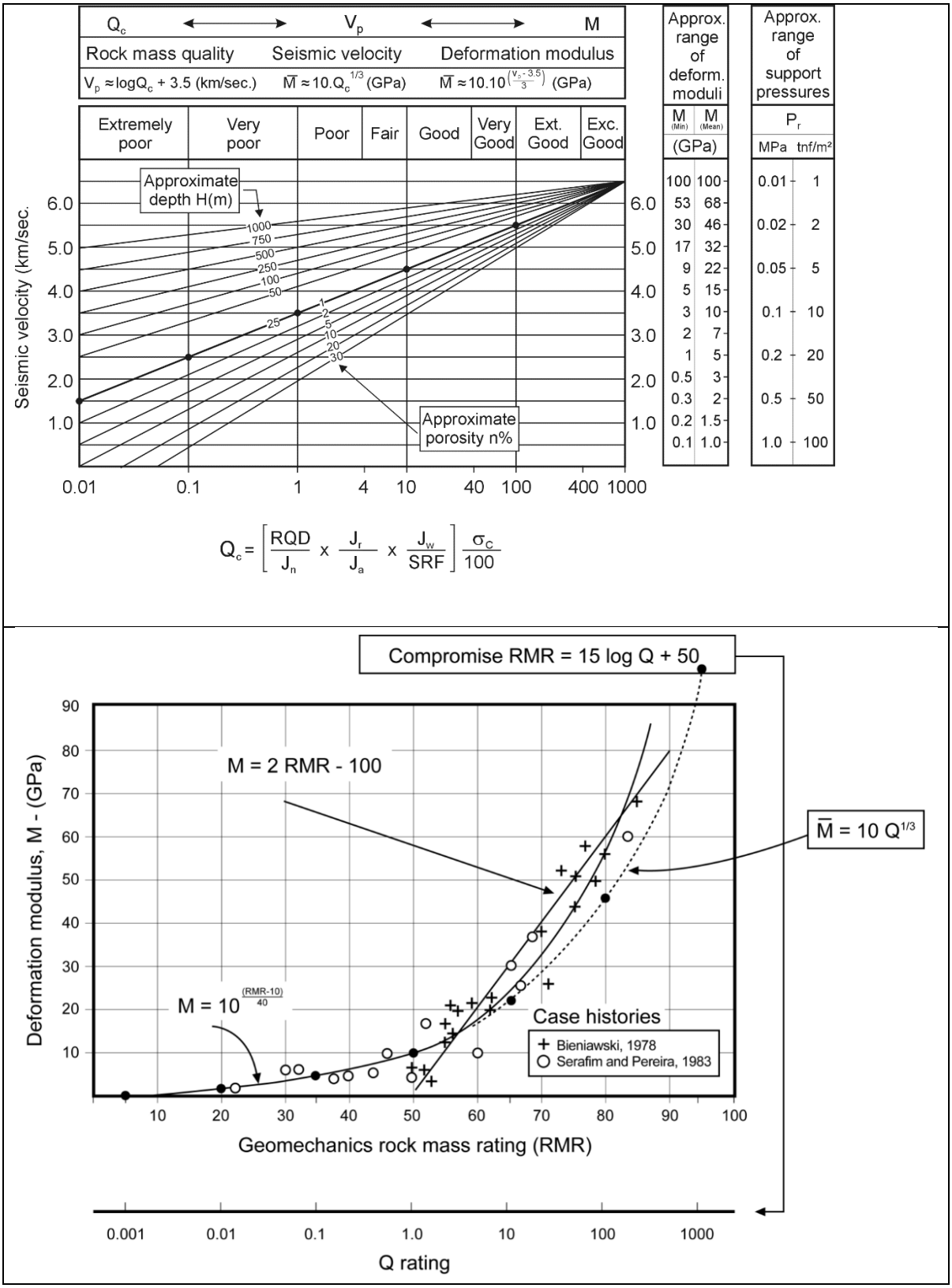

Figure 16.9 Besides Q to V_P and vice versa, the top diagram shows how to estimate the effect of increased depth on Vp (and deformation modulus M or E_{mass}). Note that support pressure (bolt plus anchor capacity for cavern support) appears to be inversely proportional to the deformation modulus estimate. The lower diagram shows the earlier Q and RMR and deformation modulus estimation, without Q_c or depth correction. Barton, 1995, 2006.

16.7 Theoretical and ‘actual’ stress redistribution around tunnels

When a tunnel is excavated, especially an idealized circular tunnel, in an even more idealised unjointed, isotropic medium (which could be an idealized massive, isotropic unjointed, elastic rock) and also subjected to vertical and horizontal stress (the latter a normal boundary condition), there occurs a redistribution of the two principal stress components to compensate for the removal of stressed material, and the need for stability of the resulting ‘excavation’. We have a tangential (or arching) stress and a radial stress. The latter reduces to near zero at the tunnel periphery. (Figure 16.10).

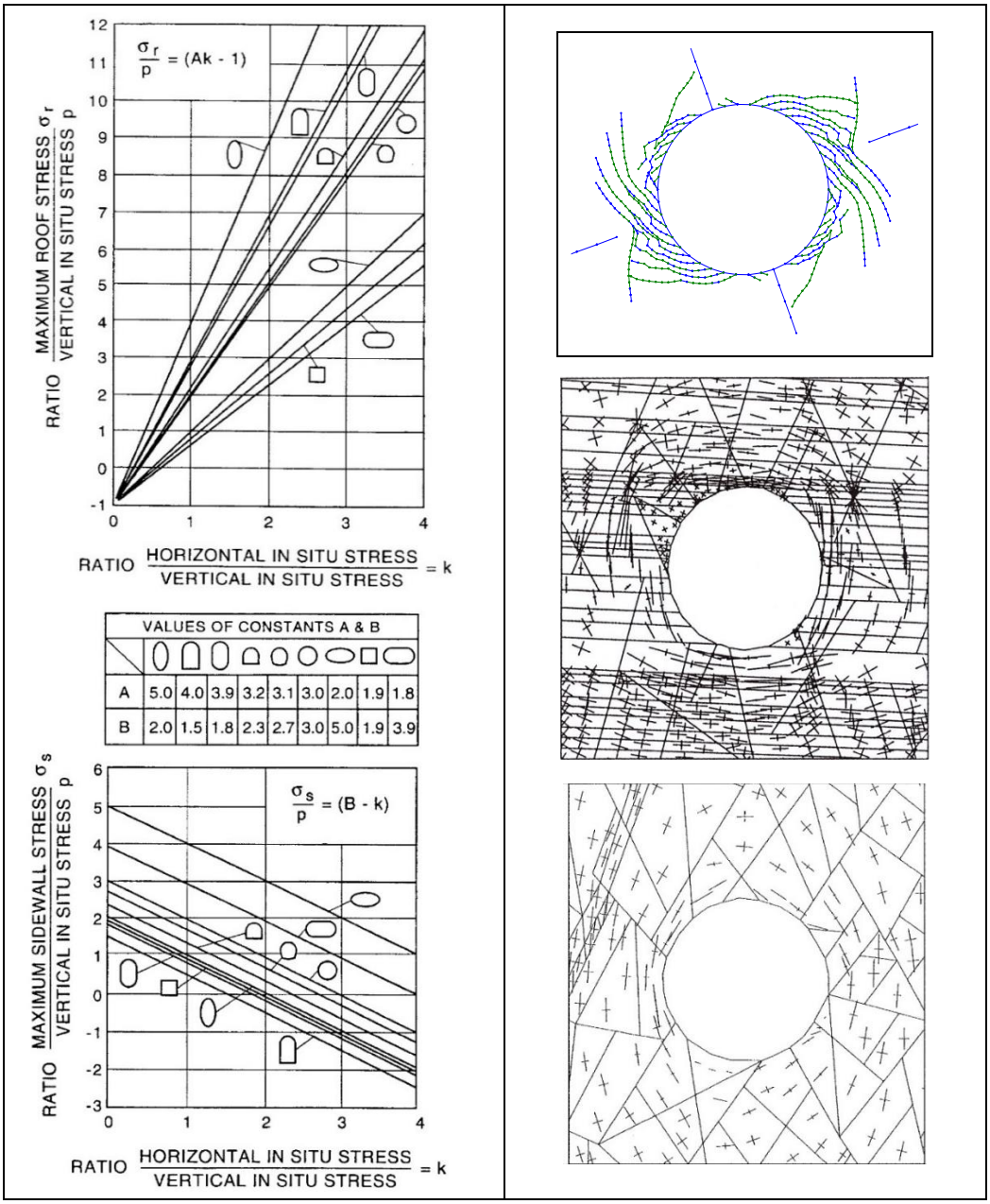

Figure 16.10 Left: Theoretical stress redistributions from Hoek and Brown. Right: UDEC-BB modelled cases from UK Nirex studies (Barton, 2000). The top tunnel illustration is from a deep highly stressed FRACOD model with log-spiral shearing (B. Shen, priv. comm.)

The theoretical stress concentration factors shown in the left side of Figure 16.10 indicate that for the case of a circular (TBM-style) tunnel, the maximum tangential stress can be expressed, following Kirsch, as $\sigma_{\theta\,max} = 3\sigma_1 - \sigma_3$ acting for instance at '6 o'clock' and '12 o'clock' if the major principal stress is horizontal prior to excavation. The minimum tangential stress after excavation, which could easily be negative, is given by $\sigma_{\theta\,min} = 3\sigma_3 - \sigma_1$. This acts at '9 o'clock' and '3 o'clock'. The 'tunnel excavations in jointed rock' (UDEC-BB models) shown on the right in Figure 16.10 indicate that the stress distributions are perturbed by local jointing, and whether it is sedimentary rock like sandstones and siltstones, or volcanic rocks like welded tuff. The bolting and shotcrete *to be selected in the next section*, which is Q-value based, ensures the stability of this stressed-and-unloaded tunnel periphery. As a curiosity since it was UNPP project based, the physical models shown in Figure 16.11 demonstrate that the deformations resulting from excavation of simulated 'reactor caverns of 50m span' depend on the rock jointing at the 'site'. With high horozontal stress and stable jointing, upwards-oriented heave is possible, as indeed can be registered in near-surface mine excavations, with pillars actually under stress-measured tension.

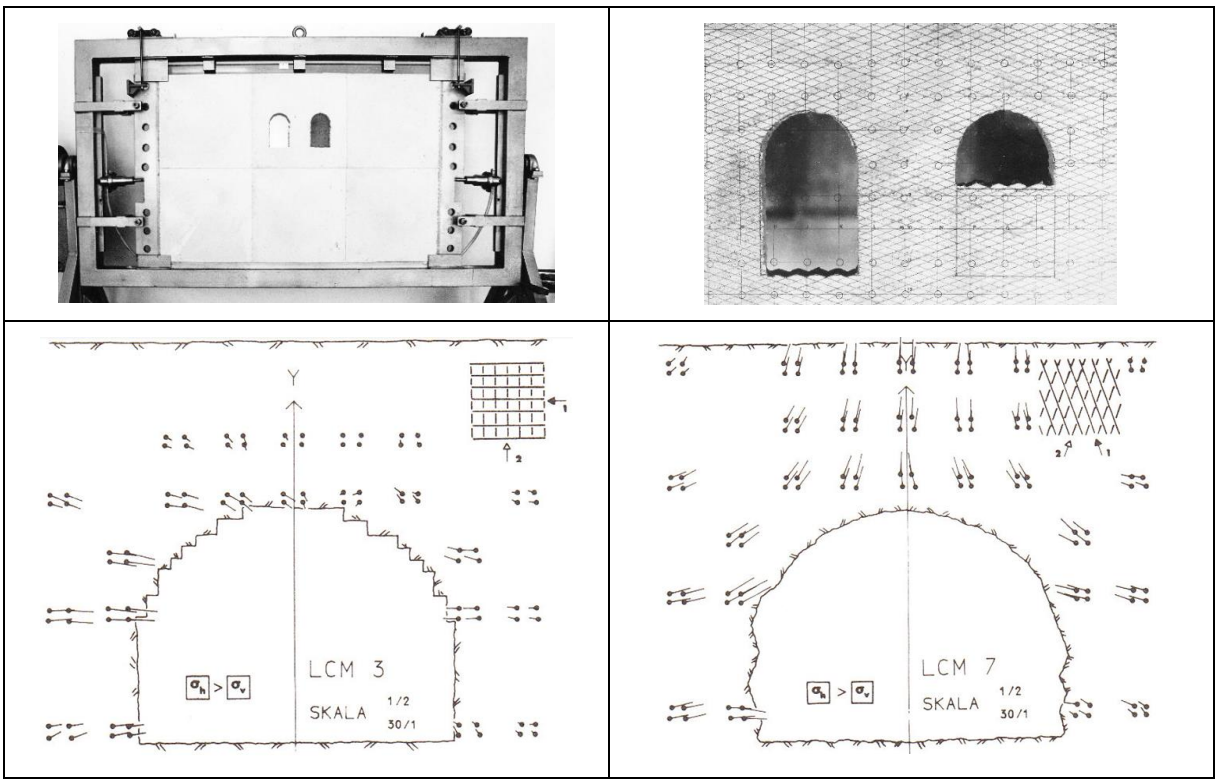

Figure 16.11 Physical models of large caverns (1976-1977) prior to the Cundall-Itasca UDEC numerical model development that dated from 1980. These physical models were performed in Norway for Statkraft, but also had Swedish financial support from BeFo as part of ***an early UNPP initiative*** *that started in the beginning of the 1970's. Photogrammetry was utilized for measurement of deformation. Two examples of single '50m' span 'reactor' caverns are shown. These had variable 'joint' anisotropy and orientation due to the intersecting (and much more uniform than in reality) tension fractures. Variable horizontal stress could also be applied: isotropic or $\sigma_h > \sigma_v$. as here. Barton and Hansteen,1979 compared these physical models with finite element FEM continuum models, finding significant differences due to the joint behaviour. This is why UDEC-BB or 3DEC are preferred to continuum models today, many years later.*

Today, in fact in the last 40 years, we have distinct element models such as 2D UDEC and 3D 3DEC, that have much greater flexibility for representing variable joint orientations, variable joint lengths, and variable input data for the shear strength and deformability of the joints. A large cavern example is shown in the next pages.

16.8 Support for tunnels and caverns, preferably Q-value based

It is time to consider the rock support needs for the tunnels and cavern complexes that will be needed for a future UNPP. As a bare minimum these will include:

- access and exit tunnels
- cooling water-in and warm water-out tunnels
  (feeding from and returning to dedicated cooling-water lagoons)
- reactor dome 'silos'
- turbine halls
- transformer halls
- bus-bar galleries
- electric cable tunnels (continuing some kilometers from the plant: so no tell-tale pylons)

A glance at one of the world's largest hydropower plants in the last pages of this chapter may convince those in doubt that underground layout complexity has already been maximised in big hydro plants, where there are several kilometers of excavations with various functions in a relatively limited area (typically 1 to 2km^2 in plan-view).

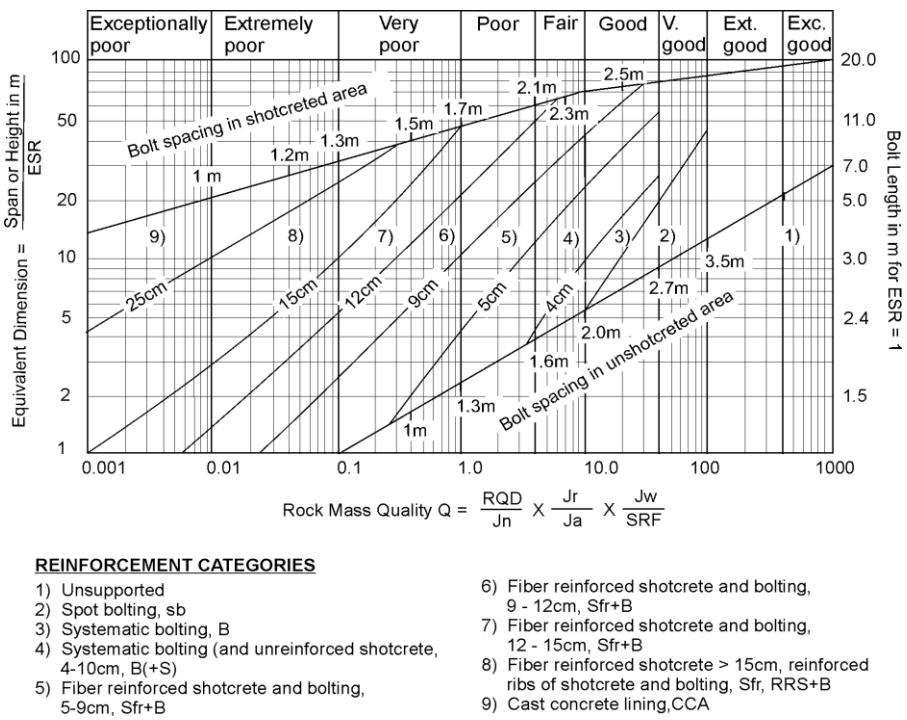

Figure 16.12 Tunnel and cavern B+S(fr) reinforcement and support based on Q-values. The ESR value that modifies span or height can be 1.0 for normal security, 0.5 for extreme. Grimstad and Barton, 1993. See also Barton and Grimstad, 1994 in Felsbau.

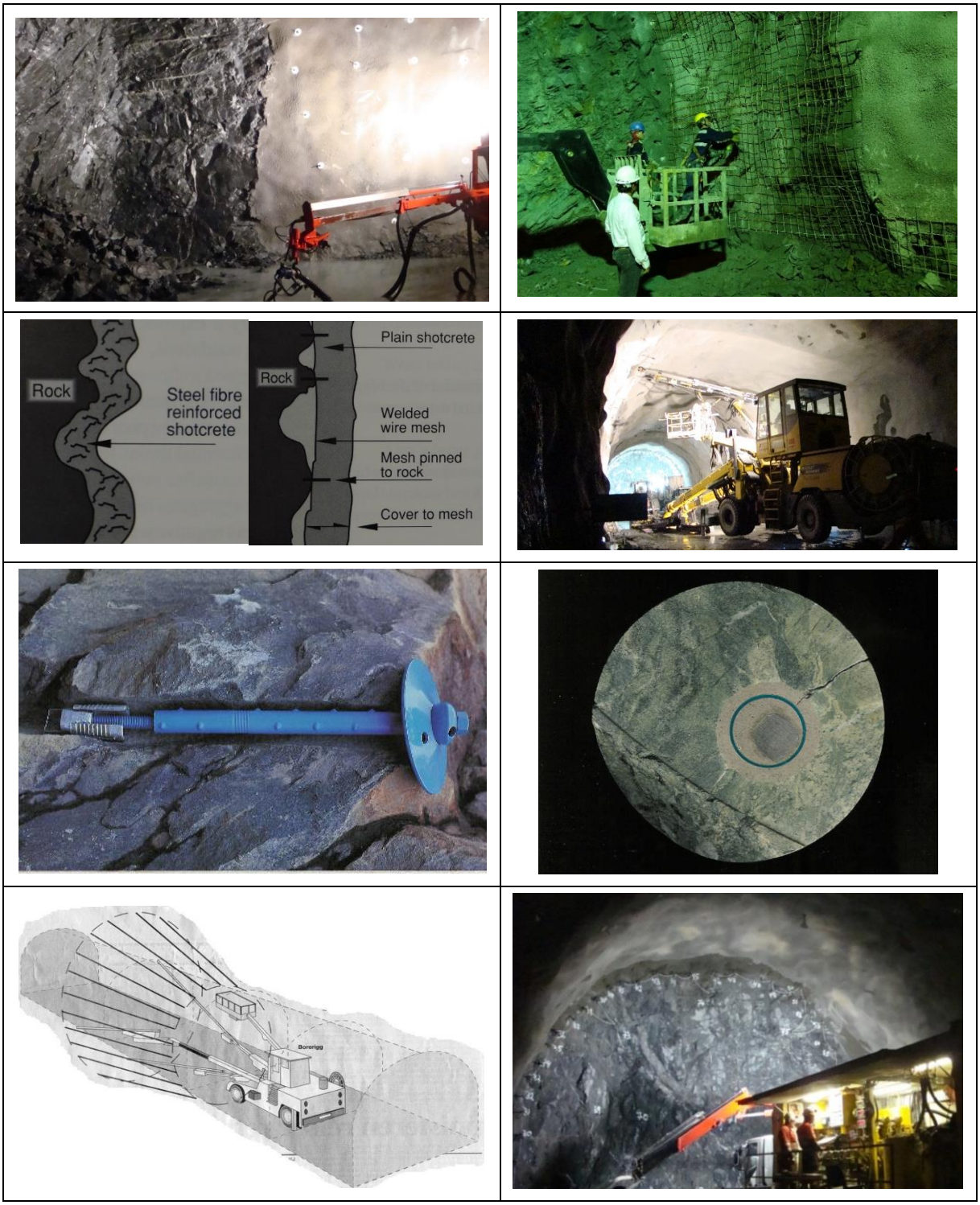

Figure 16.13 Some practical tunnelling details, from top: B+S(fr) single-shell rail tunnel, with S(fr) much preferred to the traditional S(mr) which was discontinued in Norway after 1983. Demonstration length and cored section of PVC-sleeved corrosion protected CT-rock bolt. Pre-injection umbrella principle and execution (for 5km) in the high-speed rail Bærum Tunnel.

Figure 16.12 shows the tunnel and cavern support chart based on Q-values that was published by Grimstad and Barton, 1993. It has been widely used in hydropower, mining and transport tunnel construction as a ‘single-shell’ cost effective method with

significantly lower CO_2 environmental footprint than the competing and costly double-shell (shotcrete and concrete) alternatives such as NATM. We refer to the single-shell method as NMT when based on Q-system support and reinforcement methods. Figure 16.13 illustrates two of the alternatives for steel-reinforced shotcrete. In fact polypropylene fibres are now much in favour for reinforcing the shotcrete. Fibre products with good anchorage are recommended for tunnelling since finite (mm-size) deformations may occur, and fracture energy absorption is important in the case of deeper tunnels. Concerning the major alternatives: single-shell or double-shell, Figures 16.14 a and b indicate the reasons for large time and cost (and concrete volume) differences between NMT and NATM

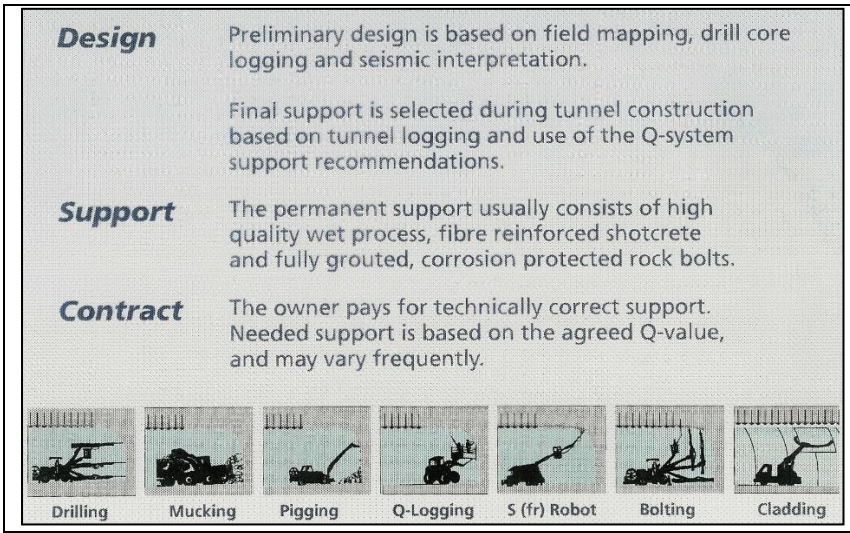

Figure 16.14 a, b. One of the cost-saving measures of NMT contra NATM is full-face excavation, though this of course is influenced by the rock mass quality. Note that most of these drawings are missing over-break which, as illustrated in Figure 16.15, may be a standard part of drill-and-blast tunnelling. In NMT over-break does need to be filled with shotcrete or concrete. In NATM it does, hence the big differences.

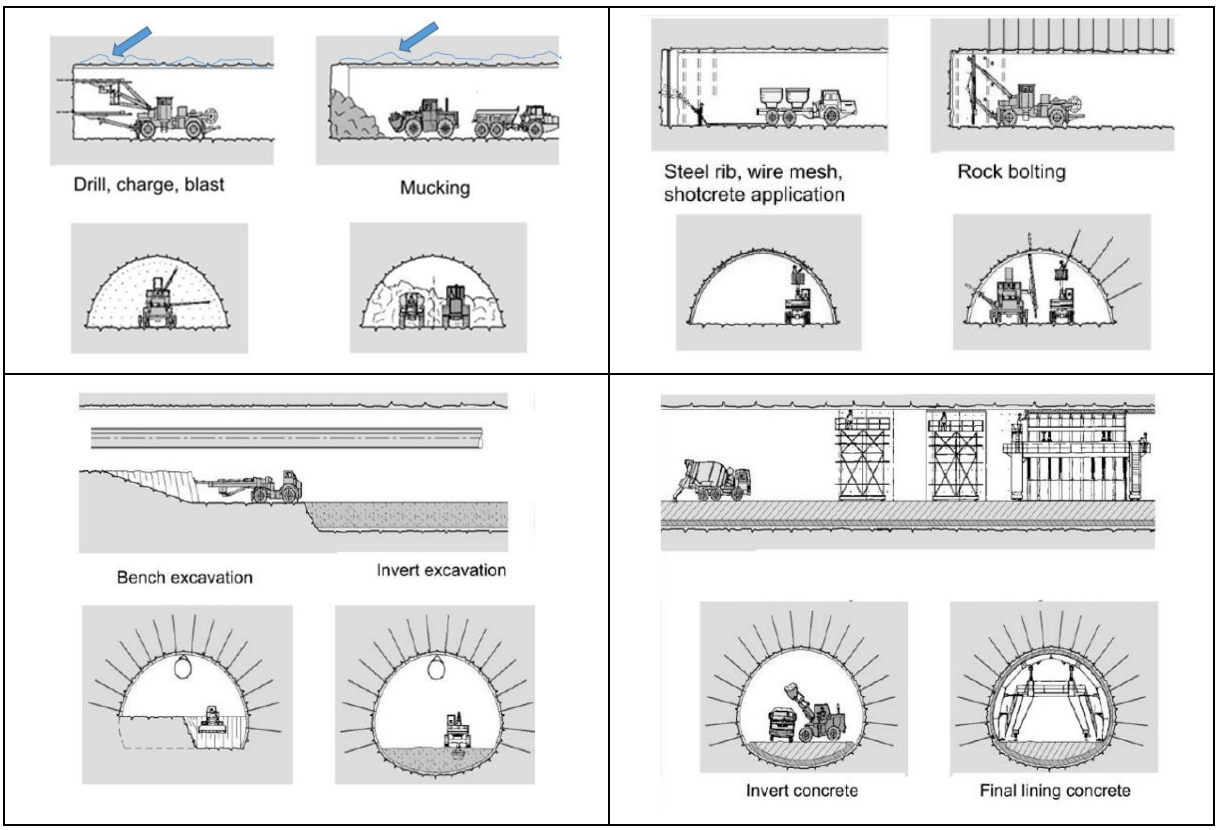

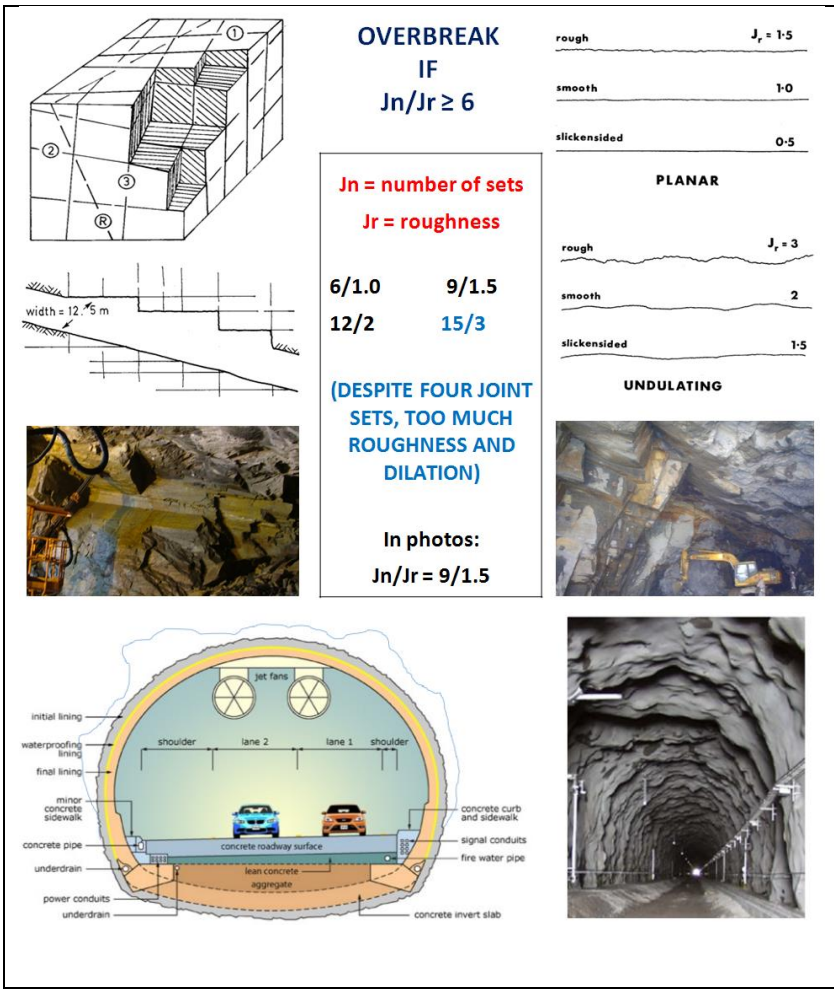

Figure 16.15 It is found that rock-joint over-break is inevitable in drill-and-blast tunnels if the ratio of Jn/Jr (number of joint sets/ joint roughness) is ≥ 6. A typical result is 9/1.5 (three sets and planar-rough-surface joints). Any clay coatings on the joints (Ja > 1) immediately guarantees over-break, likewise if the joints are planar-smooth (9/1.0). The advantage with NMT is that over-break does not have to be filled. A 'cylinder' of shotcrete is not needed for tunnel stability in moderately-to-hard jointed rock. B+S(fr) guarantees stability. The rough surface of the arch in the Gjøvik cavern, with up to 1m of overbreak, and only 10cm of S(fr) and systematic bolting (B 2.5m c/c, L = 6m was sufficient.

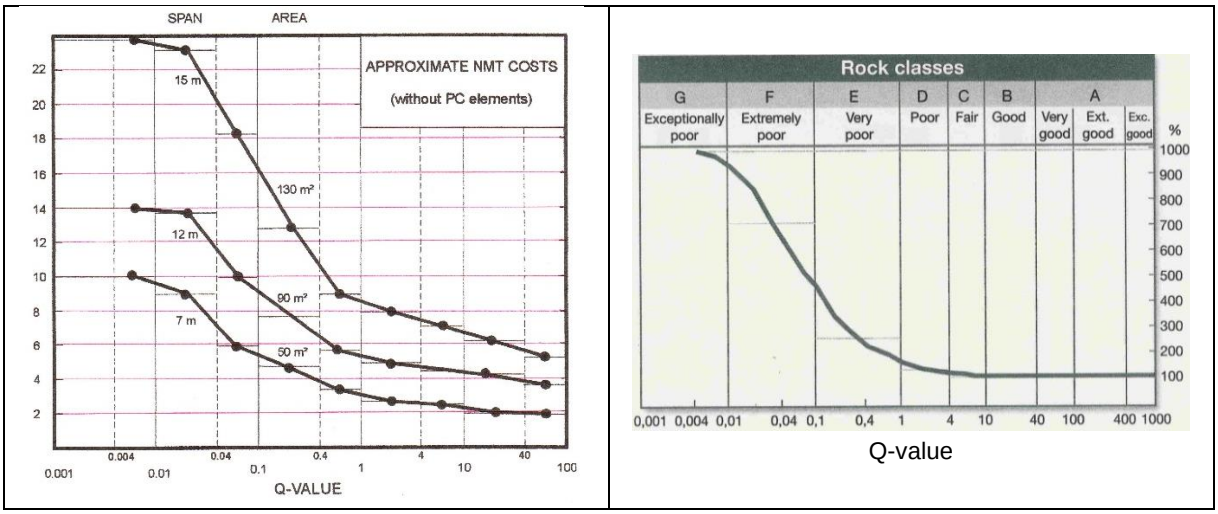

Figure 16.16 Relative cost and time for tunnelling in relation to Q-values, from Barton, 2017 and Barton, Buen and Roald, 2001. Roald's studies incorporated 50km of tunnels from Norway and Sweden. A similar-shaped but 12:1 cost difference was found. (10:1 for time as here).

16.9 Input data for realistic numerical modelling

When planning to perform distinct element models such as 2D UDEC-BB or three-dimensional 3DEC-MC (BB is the non-linear, block-size dependent Barton-Bandis joint behaviour option, which is preferred to the linear Mohr Coulomb model), it is necessary to assemble via suitable index and laboratory testing, and of course from drill-core analysis, much of the additional input data listed in Table 16.2. This table shows that the six Q-parameters represent just a part of the 'rock mass structure' and 'joint character' and 'boundary conditions' (water and stress/strength).

I	ROCK MASS STRUCTURE			
1	RQD	Deere et al., 1967)	block size	Q
2	J_n	= joint set number		Q
3	F	= joint frequency (per metre)		
4	J_v	= volumetric joint count (Palmström, 1982)		
5	S	= joint spacing (in metres)		
6	L	= joint length (in metres)		
7	w	= weathering grade (ISRM, 1978)		
8	α/ß	= dip/dip direction of joints (Schmidt diagram)		
II	JOINT CHARACTER			
9	J_r	= joint roughness number	shear strength	Q
10	J_a	= joint alteration number		Q
11	JRC	= joint roughness coefficient		
12	a/L	= roughness amplitude of asperities per unit length (mm/m)		
13	JCS	= joint wall compressive strength		
14	ϕ_r	= residual friction angle		
15	r,R	= Schmidt rebound values for joint and rock surfaces		
III	WATER, STRESS, STRENGTH			
16	J_w	= joint water reduction factor	active stress	Q
17	SRF	= stress reduction factor		Q
18	K	= rock mass permeability (m/s)		
19	σ_c	= compressive strength		
20	σ_1	= major principal stress		

Table 16.2 The six Q-system parameters RQD, Jn, Jr, Ja, Jw and SRF represent basic elements of a more complete list of input that need to be assembled for distinct element modelling. In DEM, joint sets will be represented, rather than just 'merged' into equivalent (though not sufficiently representative) isotropic continuum approximations. For UDEC and 3DEC joint geometries and joint strengths and deformabilities are needed, much of which can be obtained from the parameters JRC (#11) and JCS (#13) via the Barton-Bandis strength, stiffness and block-scaling routines. A glimpse of some of this index and shear box testing in shown in Figures 16.17 and 16.18. Note that the 3D joint geometry is traditionally represented by 'joint poles' (literally a perpendicular pole) plotted on the surface of lower half-hemisphere Schmidt nets. The concentrations of the different joint sets are represented by contoured frequency, and the resulting dips-and-dip-directions are the basis for the approximated modelled geometries.

The histograms for JRC, JCS and φ_r seen at the bottom of Figure 16.17 end up as part of a more extensive EXCEL summary spreadsheet that includes the Q-parameter statistics. Many hundreds of such spreadsheets will be generated when logging and testing joint samples from many kilometers of drill-core, as for example when NGI were assisting UK Nirex in geotechnical studies for the planned Sellafield ILW caverns repository in NW England. The spreadsheets contained the input data needed for UDEC-BB modelling of the rock-bolted caverns at 500 to 700m depth. In the case of a UNPP cavern and tunnel project, much shallower depths (100-200m) would suffice.

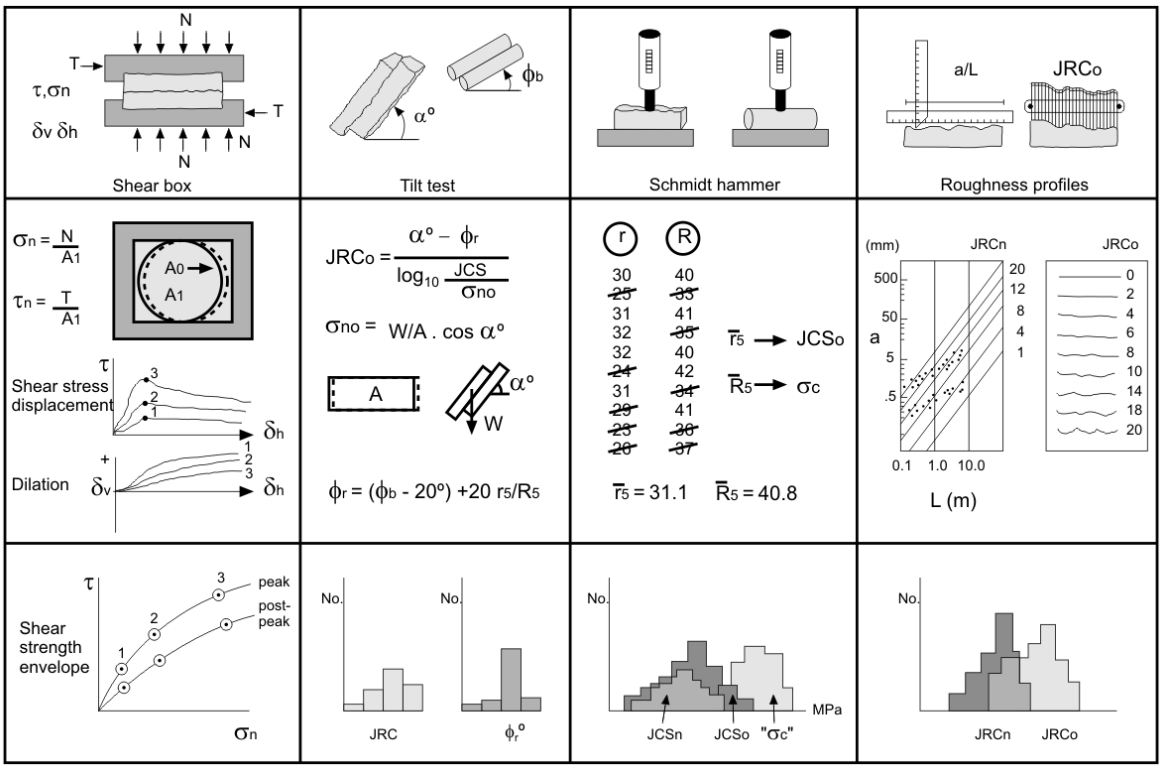

Figure 16.17 Four columns of diagrams showing 1. direct shear tests principles (Note: apply shear force T 'in-line' to avoid creating a moment), 2. tilt test principles, 3. Schmidt hammer test principles, and 4. Joint roughness recording principles. Each of these simple methods are described in Barton and Choubey, 1977 and the more recent Barton and Bandis, 2017. Note: the histograms would end up as part of a more extensive EXCEL summary spreadsheet that includes the Q-parameter statistics.

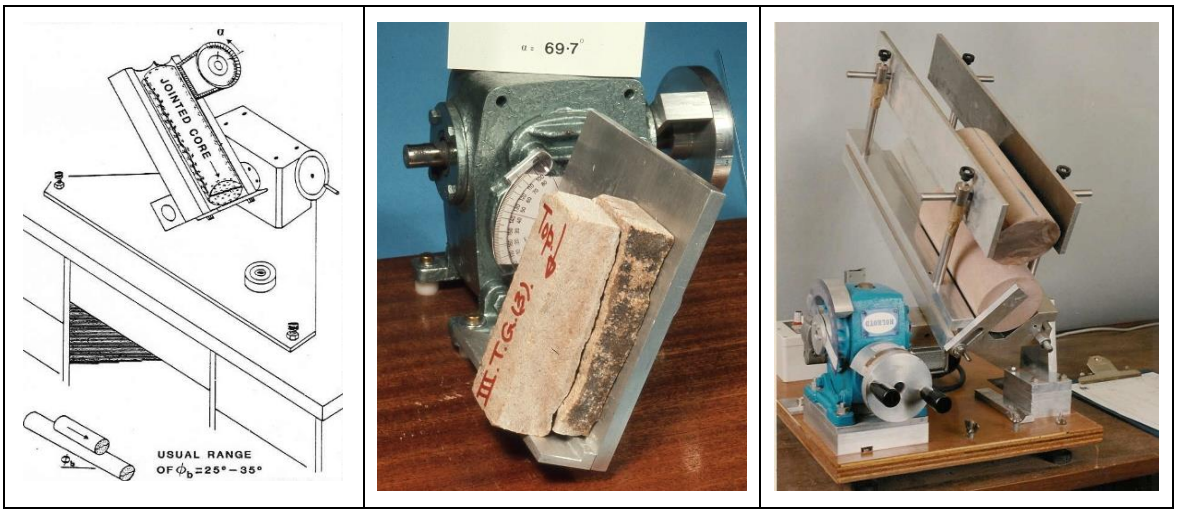

Figure 16.18 Two of the laboratory index tests for determining JRC and φ_b. Usually the joint samples will be diamond-sawn from drill-core, and some will be direct-shear tested. There will be focus on representing and testing each of the principal joint sets that are to be the basis of the jointed models, whether UDEC or 3DEC. Examples of UDEC-BB are given in the next figures. An engineering geologist approximated the 3D joint structure in 2D and his expert drawings are then digitized as a basis for the modelled geometry. Care should be taken not to exaggerate joint continuity in relation to the reality. This would accentuate modelled deformations. An empirical deformation Δmm versus Q-value is given later.

16.10 An example of large-cavern modelling and monitoring

A UDEC-BB model geometry for the Gjøvik cavern, showing the stages of numerical excavation (1 to 8) is shown in Figure 16.19. It included three additional Post Office tunnels/caverns to one side of the 60m span main cavern. 'Excavation' of these (up to 20m wide caverns caused some small modifications to the main stress 'arch' and to local bolt and anchor forces in the 'pillar' area between the caverns.

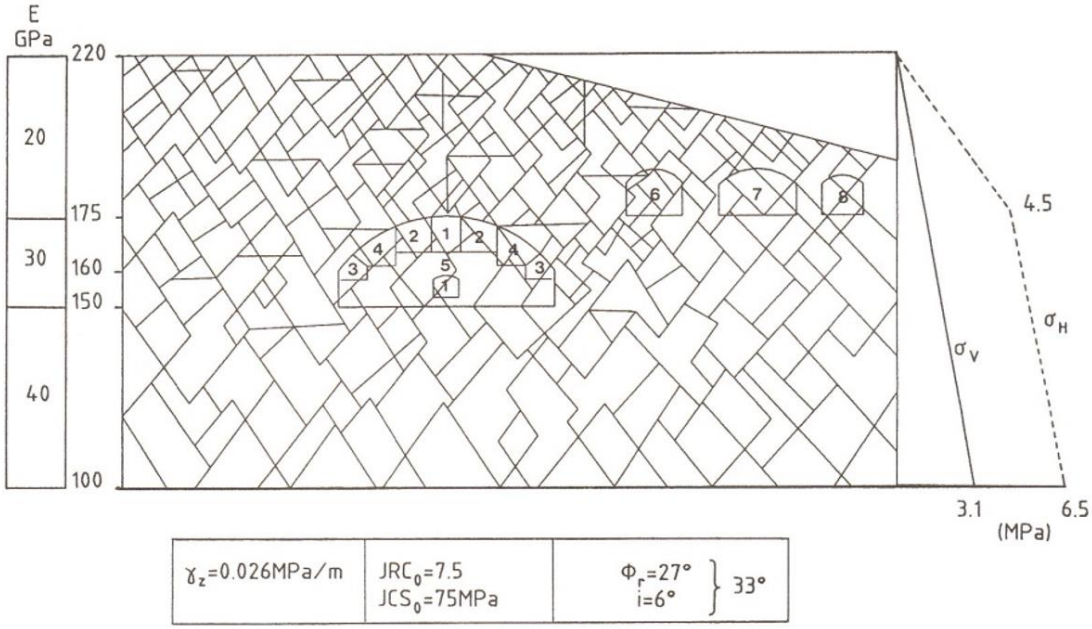

Figure 16.19 The numbers down the left-side of the UDEC model geometry show height above sea level and three depth-dependent moduli of deformation (E_{mass} or M in GPa). Below to the right side are vertical stress (gravity-based) σ_V and the estimated horizontal stress (σ_H) based on an interpretation of hydraulic fracture and joint deformation borehole test data. The input data for the numerical modelling of the joint strength and stiffness, using joint roughness JRC and wall strength JCS is shown in the boxes. A 'Patton i-value' was used to better represent the large-scale roughness of the undulating joints which were roughness profiled up to a length-scale of 2m. The options for joint strength modelling are given in Figure 16.20.

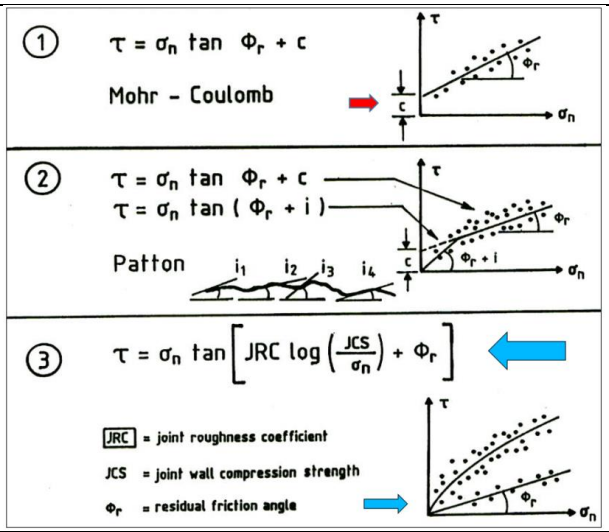

Figure 16.20 Diagrams and equations representing the most common shear strength criteria for rock joints: Mohr-Coulomb, Patton, 1966 and Barton and Choubey, 1977. This has no 'c' intercept, as only when there are steep steps do rock joints have actual cohesion. Hence 'c' is absent from equation #3. The input values of JRC and JCS also provide estimates of joint normal and shear stiffness kn and ks. These usually differ by a factor of 50:1 or even 100:1. It depends on rock-block sizes.

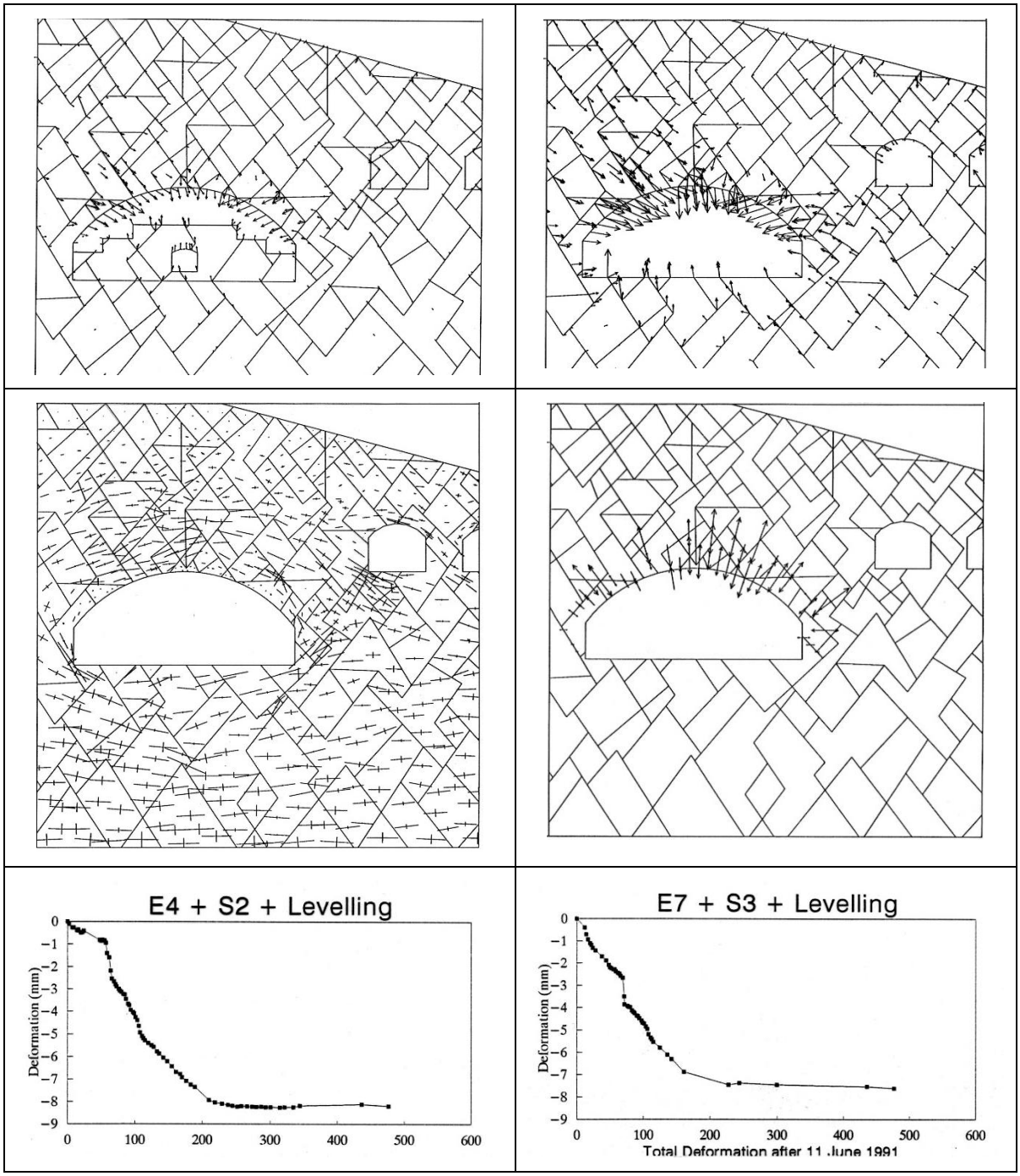

Figure 16.20 a, b: Some results of UDEC-BB modelling of the planned Gjøvik cavern excavations: maximum deformations were 6 to 8mm. c, d: Stress distribution and bolt-and-anchor forces at joint crossings. e, f: Monitoring of cavern arch deformations, using surface-installed and top-heading-installed MPBX extensometers, and surface monitoring. The measured deformations of 7 to 8 mm were very close to the numerical model predictions.

In Table 16.3 some empirically-based and very simple relationships between Q-values and tunnel and cavern deformations are given. A central trend of hundreds of data, with a huge majority provided by researchers from Taiwan, has surprisingly indicated that Δ (mm) ≈ SPAN (m) / Q. This can be used as a 'reality check'. (Barton, 2002).

World's largest top-heading waiting for benching-down.

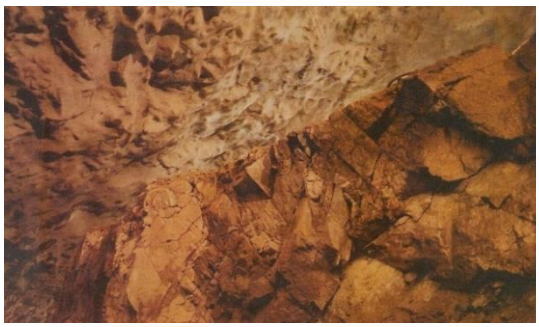

Mean 10 cm of S(fr). Note: some over-break in arch > 1 m.

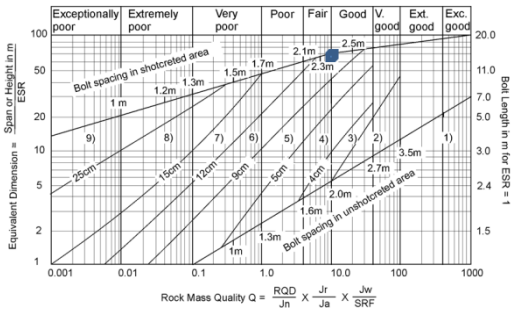

Q_{mean} ≈ 10, span 62m. B 2.5m c/c + S(fr)10cm + cables.

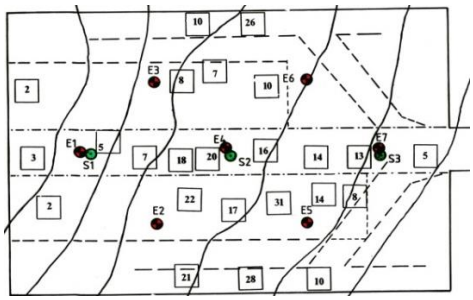

Q-values of arch (boxes): long external MPBX: in red

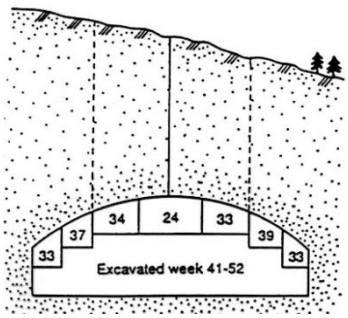

MPBX locations (three rows), excavation weeks in 1991.

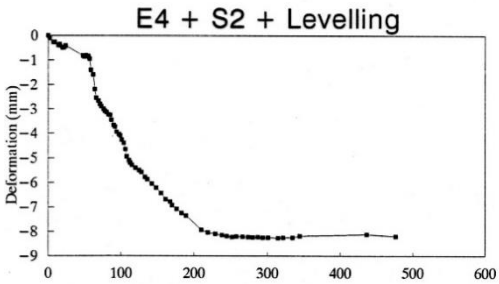

Central deformation 8 mm, ends: 7.0 mm and 7.5 mm

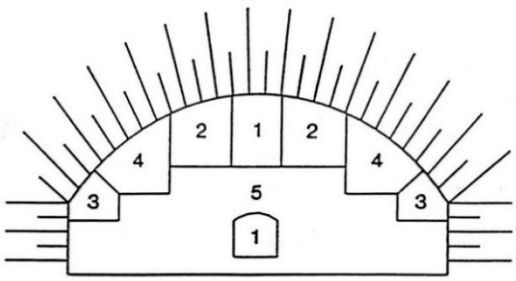

B 2.5m c/c L= 6m, + twin-strand anchors L=12m, c/c 5m

Early games: ice hockey in Winter Olympics of 1994.

Figure 16.21 The largest-span NMT project, the 62 m span Gjøvik Olympic cavern in Norway. Note moderate quality of the jointed gneiss and the local over-break in the arch of > 1m (top-right photo). Note: no lattice girders, no concrete, so no problem with over-break. A drip-shielded, drained-but-dry cavern. When water control is needed, systematic pre-injection will be performed. In the period 2005 to 2010 a total of 12km of high-speed rail tunnels (three tunnels) were systematically pre-injected in the rail corridor west of Oslo, Norway.

Table 16.3. Improved empirical equations for estimating the likely magnitudes of tunnel or cavern deformation. When using the last three equations, SPAN is expressed in mm, deformations are in mm, and stress and strength are in MPa. (Barton, 2002).

$\Delta = \frac{SPAN}{Q}$	$\Delta_v = \frac{SPAN}{100Q}\sqrt{\frac{\sigma_v}{\sigma_c}}$	$\Delta_h = \frac{HEIGHT}{100Q}\sqrt{\frac{\sigma_h}{\sigma_c}}$	$k_o = \left(\frac{SPAN}{HEIGHT}\right)^2\left(\frac{\Delta_h}{\Delta_v}\right)^2$
Nathpa Jakri power station cavern		**Gjøvik Olympic cavern**	
$\Delta_v = \frac{20{,}000}{100 \times 3} \times (6/35)^{1/2} = 28$ mm $\Delta_h = \frac{50{,}000}{100 \times 3} \times (4/35)^{1/2} = 56$ mm (SPAN = 20m, HEIGHT = 50m, Q = 3, σ_V=4 MPa, σ_h = 6 MPa, σ_C = 35 MPa). (In the middle of the range of MPBX measurements for the arch and walls).		$\Delta_v = \frac{60{,}000}{100 \times 10} \times (1/75)^{1/2} = 6.9$ mm (SPAN = 60m, Q_{mean} = 10, σ_V = 1 MPa at 40 m depth, σ_C = 75 MPa) (Almost identical to that measured with nine MPBX, and almost identical to UDEC-BB modelling results).	

16.11 Use of rock for large hydropower caverns : Baihetan HEP

This introductory text on the use of rock for underground siting of important facilities, including the present focus on post-Fukushima underground nuclear power plants (UNPP) would be largely incomplete if it did not include reference to past and recent hydropower caverns. These house expensive machinery, in some cases with greater generating power than even the world's largest (surface) nuclear power plants. For example: the Kashiwazaki-Kariwa plant in Japan is currently the world's largest nuclear power plant, with a net capacity of 7,965Mw. Nevertheless, it is dwarfed by the world's largest underground hydroelectric (twin) power plant. Baihetan HEP in China can generate 16,000MW, using 8 units of 1,000Mw in twin 438m long powerhouses under *opposite banks* of the powerful river, which runs between canyon walls.

Figure 16.22 Right-bank of the Baihetan project prior to large-scale construction. The cross-jointed and actually 'macro-cracked' columnar basalt had a tendency to degrade rapidly when unloaded. Immediate B+S(fr) was the solution, but this was delayed in some major excavations, and resulted in reported problems with over-break and rock failure. Due to the high rock stresses under the canyon walls, the stress/strength ratio (σ_θ / σ_c) was clearly unfavourable, and elevated SRF values would have been recommended if using the Q-system for tunnel and cavern support selection. Nevertheless, cavern wall heights greatly exceeded empirical data, thus requiring careful 3D numerical modelling with 3DEC.

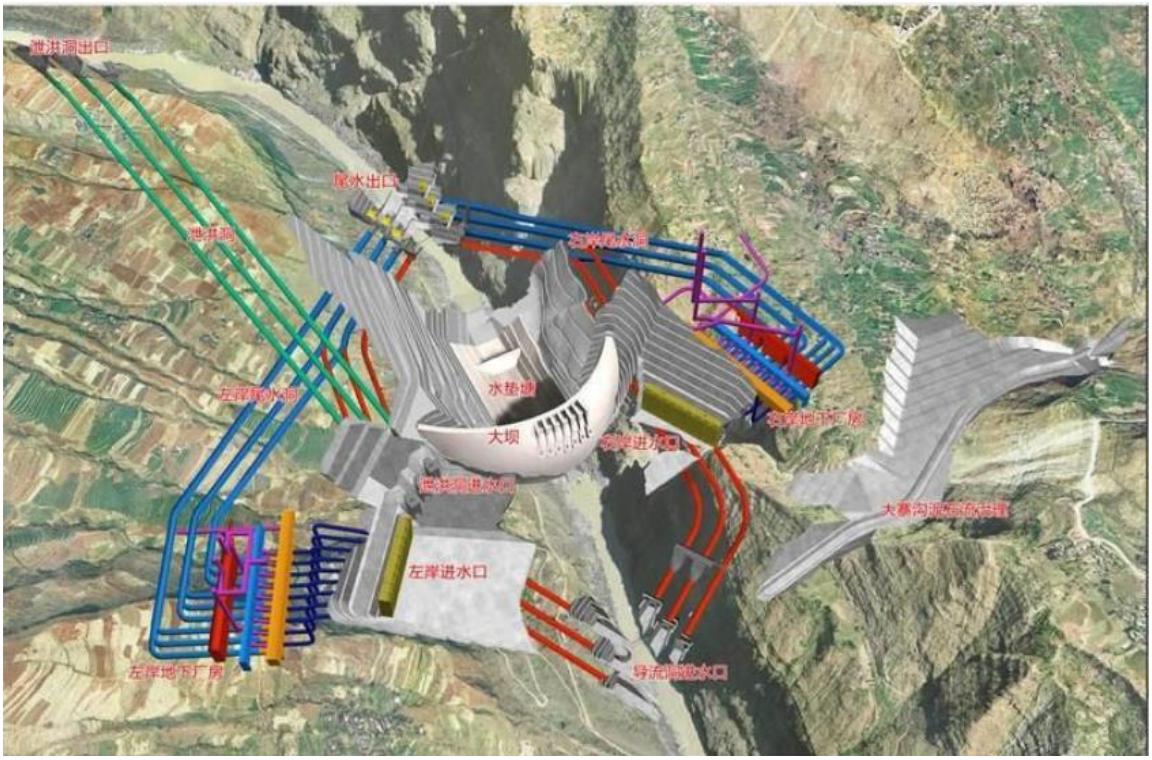

Figure 16.23 Internet pictures of the Baihetan hydroelectric project, China, showing the twin 2 x 8,000MW layout and a photograph from inside one of the caverns (with a height of > 85m). Note the shotcrete lining and concrete-protected anchor heads. The two power caverns are coloured yellow in the '3D' 'transparent rock' view in the upper figure. These are 438m long.

The rock for all six caverns is columnar basalt, which proved to be a challenge due to a tendency to loosen if not supported and reinforced in a timely manner. The rock exposed along the canyon walls was shown in Figure 16.22. The walls of these foot-paths disintegrated rapidly since without S(fr) protection, as only temporary paths.

16.12 Conclusions

1. From the point of view of rock engineering experiences from around the world, it is difficult to imagine that there could be insurmountable underground construction challenges for the siting of *nuclear power plants in rock caverns*. The heavy underground construction industry, and of course numerous reputable and highly experienced consulting companies have designed and built complex projects in rock thousands of times. Foremost in complexity are probably the 800 or more underground hydroelectric stations, which often require three parallel caverns of large volume. The machine halls housing a typical line of multiple generators have reached several hundreds of meters length, spans of more than 30m and heights in excess of 80m.

2. In the case of the Baihetan project in China, built across a fast-flowing tributary of the Yangtsi River, there are twin power plants beneath each valley (canyon) side, each with the generating capacity equal to the largest nuclear power plant in the world (TEPCO's Kashiwazaki-Kariwa plant in Japan with a net capacity of 7,965MW). Baihetan generates 2 x 8,000MW, using 16 x 1,000MW turbines. The two powerhouse caverns each measure 438m length x34m span x89m height. These are much larger in volume than will be needed for nuclear power, and they were built in rock masses of somewhat unfavourable character (columnar basalts).

3. A practical glimpse of the design checks, modelling, monitoring and construction of a cavern of even larger span (62m) but of limited height and length is given as an illustration of some of the practical issues that need to be addressed. Before the Norwegian Olympic cavern project (from the early nineties), a project for potential underground siting of a nuclear power plant was initiated in Norway (and Sweden) in the early 1970's.

4. There was initial Norwegian focus on a potential UNPP site at Brenntangen on the east side of the Oslo fjord. Various site characterization tasks were performed by NGI. Subsequently both Norway (Statkraft) and Sweden (BeFo) supported a physical model-based research project for investigating the challenges associated with 50m span reactor caverns in jointed rock. Surface construction of nuclear power plants was in the meantime initiated in Sweden, mostly in the mid-seventies and mid-eighties (Barsebäck, Ringhals, Oscarshavn, Forsmark). *No nuclear power* generation was the development option eventually chosen in Norway, due mainly to the rich sources of hydropower in this country. So there is still no UNPP in Norway after 50 years.

5. The opportunity to build a large span cavern in rock, actually for use by the sporting (or concert-going) public did eventually arise in Norway, and it was to be ready for the 1994 Winter Olympics. The initial idea was literally sketched on a proverbial restaurant napkin by Mr.Jan Rygg for the benefit of a town planner, and final design was by Fortifikasjon/Noteby, with site investigation and design checking assistance by NGI. The rock engineering construction of the 62 x 25 x 90m cavern took just seven months, by the Selmer-Veidekke JV rock group. The cavern is next to an underground swimming pool, and various civil defence caverns, on the outskirts of Gjøvik, a town in southern Norway, not far from Lillehammer – the official site of the 1994 Winter Olympic games.

6. With suitable siting the rock engineering construction costs of 10m, 20m, 30m, 50m (or even larger) excavations can be reliably estimated and their stability guaranteed by application of modern rock design and construction techniques. Adverse structural geology, such as sedimentary rock with bedding planes filled with sheared clay ('bedding-plane faults') have also been engineered on occasion and resisted major earthquakes successfully (Barton, 2021).

7. As opposed to the typical surface plant, one that is sited underground is secure from physical damage caused by hurricanes, tsunamis, earthquakes, and missile attacks or aeroplane accidents or terrorist hijacks as in '9/11'.

8. Although less likely, due to the need for longer investigation times, and more stringent siting, it is entirely likely that a chosen UNPP site of major proportions could eventually be in the same general location as a deep final 'geologic' repository for HLW. Forsmark in Sweden, and Onkalo in Finland are presently linking existing surface nuclear plants with deep HLW repositories. The granitic rock masses at both sites have quite high Q-values, and would be eminently suited for large-scale cavern construction (i.e. UNPP) if this was a future requirement.

Gjøvik cavern opening ceremony, seating 5,500. Tunnel Talk. We are sitting beneath 10cm of good quality S(fr) and 2.5m c/c rock bolts of 6m length. RQD is a moderate 60-90%, and there are three joint sets. The cavern is at 30 to 50m depth. Maximum deformation was 7 to 8m.

16.13 References

Barton, N.R., Lien, R. and Lunde, J. 1974. Engineering classification of rock masses for the design of tunnel support. Rock Mech. 6(4), 189-239.

Barton, N., Lien, R. & Lunde, J. 1977. Estimation of support requirements for underground excavations. Proc. of 16th Symp. on Design Methods in Rock Mechanics, Minnesota, 1975. pp. 163-177. ASCE, NY. Discussion pp. 234-241.

Barton, N. & Choubey, V. 1977. The shear strength of rock joints in theory and practice. Rock Mechanics 1/2:1-54. Vienna: Springer.

Barton, N. & Hansteen, H. 1979. Very large span openings at shallow depth: Deformation magnitudes from jointed models and F.E. analysis. 4th RETC; Atlanta Georgia, Vol. 2: 1131-1353. Eds Maevis and Hustrulid. Am. Inst. of Min. &, Metall., and Petr. Engrs, Inc. New York.

Barton, N. 1995. The influence of joint properties in modelling jointed rock masses. Keynote Lecture, 8th ISRM Congress, Tokyo, 3: 1023-1032, Balkema, Rotterdam.

Barton, N. 2000. *TBM Tunnelling in Jointed and Faulted Rock*. 173p. Balkema, Rotterdam.

Barton, N. 2006. *Rock Quality, Seismic Velocity, Attenuation and Anisotropy.* Taylor & Francis, UK & Netherlands, 729 p.

Barton, N., By, T.L., Chryssanthakis, P., Tunbridge, L., Kristiansen, J., Løset, F., Bhasin, R.K., Westerdahl, H. & Vik, G. 1994. Predicted and measured performance of the 62m span Norwegian Olympic Ice Hockey Cavern at Gjøvik. Int. J. Rock Mech, Min. Sci. & Geomech. Abstr. 31:6: 617-641. Pergamon.

Barton, N. 2017. Minimizing the Use of Concrete in Tunnels and Caverns – Comparing NATM and NMT. Keynote lecture, GeoMEast2017 Int. Conf. on Sustainable Civil Infrastructures (SCI): Innovative Infrastructure Geotechnology. Sharm El-Sheikh, Egypt, 36p.

Barton, N.R. and S.C. Bandis, 2017. Characterization and modelling of the shear strength, stiffness and hydraulic behaviour of rock joints for engineering purposes. Rock Mechanics and Engineering, Ed. Xia-Ting Feng, Vol. 1, Principles. Ch. 1, 3-40. Taylor & Francis.

Barton, N. and Quadros, E. 2019. Understanding the need for pre-injection from permeability measurements: What is the connection? J. of Rock Mechanics and Geotechnical Engineering.

Barton, N. 2021. Application of the Q-system to tunnels and caverns in weak or faulted rock. *Fifth symposium of the Macedonian Association for Geotechnics,* ISRM specialized conference. Eds. S. Ćorić and J. Papić. Keynote lecture, 26p.

Bieniawski, Z.T. 1989. Engineering rock mass classifications: A complete manual for engineers and geologists in mining, civil and petroleum engineering, J. Wiley, 251p.

Grimstad, E. & Barton, N. 1993. Updating of the Q-System for NMT. Proceedings of the International Symposium on Sprayed Concrete - Modern Use of Wet Mix Sprayed Concrete for Underground Support, Fagernes, 1993, (Eds Kompen, Opsahl and Berg. Norwegian Concrete Association, Oslo, pp. 46-66.

Hoek, E. and Brown, E. 1980. Underground excavations in rock. Institution of Mining and Metallurgy, 527p.

Panda, M. K., S. Mohanty, B.M.P. Pingua & A.K. Mishra, 2014. Engineering geological and geotechnical investigations along the headrace tunnel in Teesta Stage-III hydroelectric project, India. *Engineering Geology 181 (2014)* 297-308.

Rehman, H., A. M. Naji, K. Nam, A. Saeed, M. Khan and H-K. Yoo, 2021. Impact of Construction Method and Ground Composition on Headrace Tunnel Stability in the Neelum–Jhelum Hydroelectric Project: A Case Study Review from Pakistan. *Appl. Sci.* 2021, *11*(4), 1655.

Sjøgren, B., Øfsthus, A. & Sandberg, J. 1979. Seismic classification of rock mass qualities. *Geophys. Prospect.*, *27*: 409–442.

Sjøgren, B. 1984. *Shallow refraction seismics*, London, Chapman & Hall. 268p.